

Out-of-equilibrium percolation transitions at finite critical times after quenches across magnetic first-order transitions

Andrea Pelissetto,¹ Davide Rossini,² and Ettore Vicari³

¹*Dipartimento di Fisica dell'Università di Roma "La Sapienza" and INFN, Sezione di Roma, P.le Aldo Moro 5, I-00185 Roma, Italy*

²*Dipartimento di Fisica dell'Università di Pisa and INFN, Largo Pontecorvo 3, I-56127 Pisa, Italy*

³*Dipartimento di Fisica dell'Università di Pisa, Largo Pontecorvo 3, I-56127 Pisa, Italy*

(Dated: March 16, 2026)

We show that an out-of-equilibrium percolation transition occurs after quenching ferromagnetic Ising-like systems across their magnetic first-order transitions. As a paradigmatic example, we consider a two-dimensional Ising system driven across its low-temperature first-order transition line by a quench of the magnetic field h from $h_i < 0$ to $h > 0$. In the thermodynamic limit and for finite values of h , the post-quench evolution under a purely relaxational dynamics is characterized by a dynamic transition at a finite critical time $t_c(h)$ from the metastable negatively magnetized phase to the positive one, marked by the percolation of the largest clusters of positive and negative spins. This out-of-equilibrium percolation transition displays a finite-size scaling behavior as in the standard random-percolation case. However, while the fractal dimension of the percolating clusters is consistent with the random-percolation value, the exponent controlling the approach to criticality differs and depends on h . We also show that the percolation critical behavior is related to the spinodal-like behavior of the magnetization in the small- h limit, which implies that the percolation time $t_c(h)$ exhibits a spinodal-like exponential dependence on h .

Percolation transitions are a cornerstone of statistical physics, appearing across diverse fields, ranging from physics and chemistry to, e.g., biology, ecology, and social sciences [1–3]. The standard percolation theory was developed within the framework of lattice models—more broadly, systems defined on graphs—in which sites or bonds are occupied with some given probability p . As p is increased, one reaches a threshold p_c at which the occupied (or activated) bonds form a percolating cluster, whose properties mirror those of statistical systems undergoing continuous phase transitions [4–8]. If the activation probabilities of each site are independent, one recovers the paradigmatic random percolation (RP) model, for which rigorous exact results are available (see, e.g., Refs. [9, 10]), and which can be mapped onto the q -state Potts models in the formal limit $q \rightarrow 1$ [11], allowing us to reinterpret the geometric transition as a standard one in a spin system. Percolation also emerges in dynamic protocols when sites or bonds are reversibly added according to a stochastic procedure [12]. If the dynamic rules are local, the system develops RP transitions as well.

In this paper we show that out-of-equilibrium percolation transitions can emerge within dynamic, local, and reversible physical protocols, in which a ferromagnetic system is driven across a magnetic first-order transition. We focus on the behavior of the paradigmatic two-dimensional (2D) Ising model, when it is driven across its low-temperature first-order transition line at zero magnetic field. In particular, we analyze the out-of-equilibrium relaxational dynamics after quenching the external magnetic field h at fixed temperature. Starting from negatively magnetized configurations, corresponding to equilibrium states for $h < 0$, the system evolves in the presence of a positive fixed $h > 0$, effectively crossing the magnetic first-order transition line. At a finite

critical time t_c after the quench, an out-of-equilibrium transition occurs, which is marked by the percolation of the largest clusters, and is related to the passage from the metastable negatively magnetized phase to the stable positively magnetized one. However, some critical features of this percolation transition differ from those the standard RP transition.

It is worth mentioning that non-RP percolation transitions have already been obtained by devising particular nonlocal and irreversible dynamic rules in some network models, such as the explosive percolation (EP) transitions [13–35]. Note, however, that the deviations from RP observed in EP transitions are essentially related to the *ad hoc* nonlocal nature of the chosen dynamics. On the other hand, in the percolation transitions considered here, the dynamics is local, but the difference with RP stems from the inherent out-of-equilibrium nature of the quenching process across first-order transitions [36–46]. This shows that non-RP transitions can also emerge in physical systems driven across first-order transitions by physically realizable local dynamics.

We consider the 2D nearest-neighbor Ising model

$$H(\beta, h) = -\beta \sum_{\mathbf{x}, \mu} s_{\mathbf{x}} s_{\mathbf{x}+\hat{\mu}} - h \sum_{\mathbf{x}} s_{\mathbf{x}}, \quad s_{\mathbf{x}} = \pm 1, \quad (1)$$

on a square lattice of size L and $V = L^2$, with periodic boundary conditions. The line $\beta > \beta_c = \ln(1 + \sqrt{2})/2$ at $h = 0$ is a first-order transition line, where the infinite-volume magnetization $M = \langle \sum_{\mathbf{x}} s_{\mathbf{x}} \rangle / V$ is discontinuous, varying between $-M_0$ and $+M_0$ for $h = 0^-$ and $h = 0^+$ respectively, with $M_0 = [1 - (\sinh 2\beta)^{-4}]^{1/8}$ [47].

We analyze the evolution arising from a sudden quench of the magnetic field across the $h = 0$ first-order transition line, at fixed $\beta > \beta_c$. The quenching protocol starts

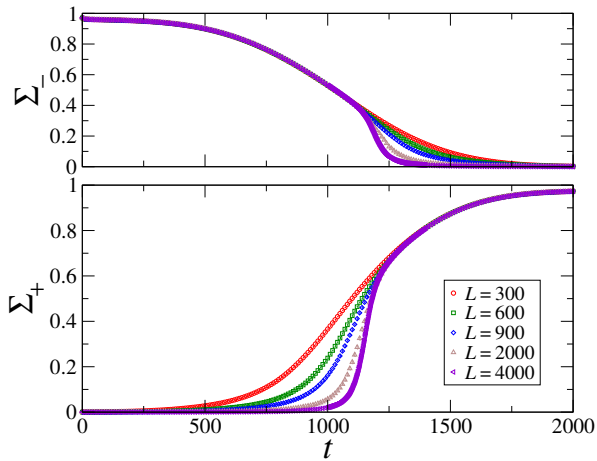


FIG. 1: The rescaled average sizes Σ_+ (bottom) and Σ_- (top) of the largest clusters of positive and negative magnetization, defined in Eq. (3), as a function of the post-quench time t , for $h = 0.07$ and several sizes L . Statistical errors are not visible, as they are smaller than the symbol size.

at $t = 0$ from equilibrated negatively magnetized configurations at $\beta > \beta_c$, effectively corresponding to $h_i = 0^-$. Then, the system evolves under a heat-bath dynamics (a specific example of local relaxational dynamics [36]) with $h > 0$. A time unit corresponds to a complete lattice sweep. See App. A 1, for details. The evolution is monitored by the magnetization

$$M(t) = \frac{1}{V} \left\langle \sum_{\mathbf{x}} s_{\mathbf{x}} \right\rangle_t, \quad (2)$$

where the average is taken over the starting equilibrium configurations and the post-quench trajectories at fixed time t . The percolation nature of the dynamic transition is probed by looking at clusters of equally oriented spins. For each configuration, clusters with positive (negative) magnetization are the connected components of the subset \mathcal{B}_+ (\mathcal{B}_-) of lattice links $\langle \mathbf{x}\mathbf{y} \rangle$ such that $s_{\mathbf{x}} = s_{\mathbf{y}} = 1$ ($s_{\mathbf{x}} = s_{\mathbf{y}} = -1$). They are determined using the Hoshen-Kopelman algorithm [48]. The size of each cluster is defined as the number of sites belonging to it. We focus on the fixed-time averages of the sizes S_+ and S_- of the largest clusters of positive and negative magnetization,

$$\Sigma_{\pm}(t) = \frac{\langle S_{\pm} \rangle_t}{V}, \quad R_s(t) = \frac{\langle S_- \rangle_t}{\langle S_+ \rangle_t}. \quad (3)$$

We report data at $\beta = 1.2\beta_c$ (results do not qualitatively change for other β , as far as $\beta > \beta_c$) and some $h > 0$. For each h , we perform simulations for several sizes $L \leq 4000$, generating a large number of independent trajectories, between 2000 (for the largest systems) and 50000, which allow us to compute $M(t)$ and $\Sigma_{\pm}(t)$.

In Fig. 1 we report $\Sigma_{\pm}(t)$ for $h = 0.07$ and several values of L . We recognize two different regimes: a small- t regime where none of the positively magnetized clusters fills a finite volume fraction of the lattice, while a fraction

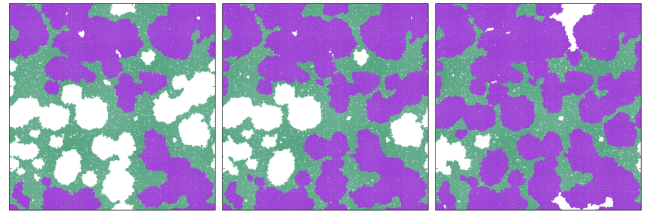


FIG. 2: Snapshots of the configurations for $h = 0.07$ and $L = 1000$, at times $t = 1144$ (left), $t = t_c = 1174$ (center), and $t = 1204$ (right). Violet and green sites belong to the largest clusters of positive and negative spins, respectively; white areas correspond to smaller (positive and negative) clusters. The size of the largest positive cluster is 368001 for $t = 1144$, 498264 for $t = t_c = 1174$, and 637204 for $t = 1204$. Its growth is due to the merging with smaller clusters, since the boundaries of the clusters are essentially unchanged.

of the volume belongs to a single negatively magnetized percolating cluster; a large- t regime where the opposite occurs, with a single positively magnetized percolating cluster coexisting with small negatively magnetized domains. They are separated by a simultaneous sharp variation of both $\Sigma_+(t)$ and $\Sigma_-(t)$, which becomes sharper with increasing L , at a transition time $t_c \approx 1200$. As t increases across t_c , positive-spin clusters aggregate very rapidly, forming a single large cluster, while the large negative-spin clusters disappear. Fig. 2 shows a sketch of the typical rapid evolution of the configurations around the transition time t_c . We have obtained analogous outcomes for other values of h , such as $h = 0.06, 0.05, 0.045$.

These results suggest that the percolation of positive clusters and inverse percolation of the negative clusters occurs at the same finite time t_c (this is likely a peculiar feature of 2D systems). In this case, $\Sigma_{\pm}(t)$ should have the typical finite-size scaling (FSS) behavior at percolation transitions [1–3],

$$\Sigma_{\pm}(t, L) \approx L^{\delta_{\pm}} \mathcal{F}_{\pm}(X), \quad X = (t - t_c)L^w, \quad (4)$$

where $\delta_{\pm} \equiv d - d_{\pm} = 2 - d_{\pm}$ (d is the dimension of the system), d_{\pm} are the critical fractal dimensions of the clusters, and the exponent w controls the approach to criticality. The numerical results for the ratio R_s also indicate that $d_+ = d_-$. Indeed, as shown in Fig. 3, they appear to scale as

$$R_s(t, L) \equiv \frac{\Sigma_-(t, L)}{\Sigma_+(t, L)} \approx \mathcal{F}_R(X). \quad (5)$$

Since $R_s \rightarrow \infty$ for $t < t_c$ and $R_s \rightarrow 0$ for $t > t_c$, the above scaling behavior implies that curves for different L cross at a finite time, which converges to the critical time t_c of the percolation transition in the large- L limit (resembling the behavior of the Binder parameter in standard spin models [8]). This is clearly visible in Fig. 3, where the R_s data for different L cross at a finite time $t_c \approx 1174$. Straightforward fits to

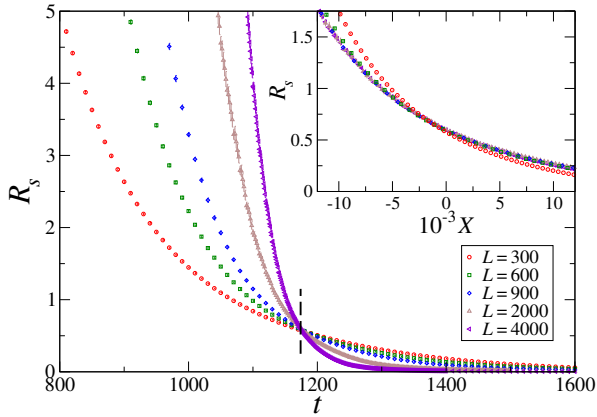


FIG. 3: The time dependence of the ratio R_s for $h = 0.07$. The vertical dashed line corresponds to the critical time $t_c = 1174$. The inset shows R_s vs $X = (t - t_c)L^w$, with $w = 0.68$. The excellent collapse of the curves (in particular for $L > 600$) supports the Ansatz (5), confirming the equality $d_+ = d_-$ of the fractal dimensions of positive and negative clusters.

the Ansatz (5), implemented through low-order polynomial interpolations of $\mathcal{F}_R(X)$, lead to the estimates $t_c = 1174(1)$ and $w = 0.680(15)$ (see Table I). The inset of Fig. 3 demonstrates the quality of the data collapse obtained using these estimates. Analogous FSS behaviors can be found for other values of h (as an example, the scaling plot for $h = 0.045$ is shown in App. A 2). The corresponding estimates of t_c and w are reported in Table I. The exponent w depends on h and differs from the RP value $w_{\text{RP}} = 3/4$ [9, 10]. Moreover, it decreases as h is reduced, suggesting that it vanishes when $h \rightarrow 0$. As a consequence, the time window Δt over which the system changes phase, which scales as L^{-w} , broadens as $h \rightarrow 0$. This behavior is consistent with the progressive slowing down of the dynamics as h decreases.

The fractal-dimension exponent $\delta \equiv \delta_+ = \delta_-$ can be obtained by matching the data for $\Sigma_{\pm}(t)$ [see Eq. (3)] with the asymptotic FSS behavior in Eq. (4). Since $\mathcal{F}_R(X)$ is monotonically decreasing, we can express X as a function of R_s by inverting Eq. (5), and write

$$\Sigma_{\pm}(t, L) \approx L^{-\delta} \tilde{\mathcal{F}}_{\pm}(R_s), \quad (6)$$

in which only δ appears. Standard fits to Eqs. (4) and (6) lead to the estimates reported in Table I, which vary little around $\delta \approx 0.10$. Notice that these estimates do not account for possible systematic deviations due to scaling corrections. Such corrections become more pronounced as h decreases and may induce deviations larger than the quoted errors. Remarkably, the numerical values of δ are very close to the RP exponent $\delta_{\text{RP}} = 5/48 \approx 0.104$ [1, 9]. This suggests that the geometric properties of the critical clusters may exhibit an h -independent universal behavior, and that the value of δ coincides with δ_{RP} . To test this hypothesis, we perform a consistency check. We fix $\delta = \delta_{\text{RP}}$ for all values of h and we verify that the FSS function $\tilde{\mathcal{F}}_{\pm}(R_s)$ obtained by $L^{\delta_{\text{RP}}}\Sigma_{\pm}(t, L)$ is universal

TABLE I: Estimates of t_c , w , δ , $\sigma_c = h(\ln t_c)^2$ and $\hat{\sigma}_c = (\sigma_c - \sigma_*)h^{-\theta}$ [using $\theta = 0.64(4)$ and $\sigma_* = 3.03(3)$]. The errors take also into account the spread of the results when varying the minimum size allowed in the fit, the data interval considered, and the degree of the polynomial interpolation used for the scaling functions.

h	t_c	w	δ	σ_c	$\hat{\sigma}_c$
0.07	1174(1)	0.680(15)	0.106(4)	3.497(1)	2.56(4)
0.06	1987(3)	0.64(2)	0.106(10)	3.460(1)	2.61(5)
0.05	3904(3)	0.56(2)	0.094(6)	3.419(1)	2.65(6)
0.045	5921(3)	0.52(2)	0.089(9)	3.395(1)	2.66(7)

up to a multiplicative h -dependent normalization factor. As shown in Fig. 4, the resulting data nicely collapse, confirming that the scaling properties are h -independent and consistent with those of standard RP critical clusters, even though the approach to the transition, most notably the exponent w , retains a nontrivial dependence on h .

We now focus on the behavior of the magnetization $M(t)$ in the thermodynamic limit (see App. A 2, for a discussion of its determination from finite-size data). For finite values of h , its post-quench evolution does not display finite-time singularities. However, a singular scaling behavior emerges for $h \rightarrow 0$. Indeed, as discussed in App. A 3, assuming that droplet nucleation is the relevant mechanism up to the critical time where the phase change occurs, the infinite-volume magnetization $M_{\infty}(t)$ is expected to scale as

$$M_{\infty}(t, h) \approx \mathcal{M}_{\infty}(\sigma), \quad \sigma = h(\ln t)^{d/(d-1)} = h(\ln t)^2. \quad (7)$$

This is confirmed by the numerical data. As shown in Fig. 5, the data of $M_{\infty}(t, h)$ corresponding to different values of h get closer and closer as a function of σ as h decreases. Moreover, the curves cross at $\sigma_* \approx 3.0$. For σ

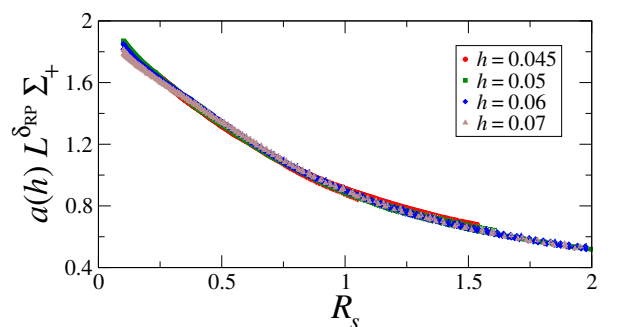


FIG. 4: Plot of $a(h)L^{\delta_{\text{RP}}}\Sigma_+$ vs R_s for various h , where $a(h)$ is chosen to optimize the collapse of the data: Setting $a = 1$ for $h = 0.045$, we use $a = 1.137, 1.096, 1.037$ for $h = 0.07, 0.06, 0.05$, respectively. We report results for $L = 2000$ (empty symbols) and $L = 4000$ (filled symbols). The resulting scaling is good, with small deviations that can be explained by residual scaling corrections.

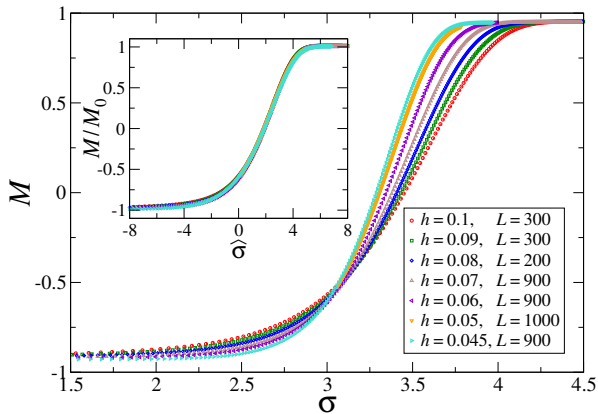


FIG. 5: The magnetization $M(t)$ plotted vs $\sigma = h(\ln t)^2$. The size L is large enough that the data can be regarded in their thermodynamic limit. The inset shows the ratio $M(t)/M_0$ vs $\hat{\sigma} = (\sigma - \sigma_*)h^{-\theta}$ with $\theta = 0.64$ and $\sigma_* = 3.03$, where $M_0 \approx 0.940259$ is the spontaneous magnetization for $\beta = 1.2\beta_c$.

close to σ_* , data show an additional scaling behavior,

$$M_\infty(t, h) \approx \widetilde{M}_\infty(\hat{\sigma}), \quad \hat{\sigma} = (\sigma - \sigma_*)h^{-\theta}, \quad (8)$$

where $\theta > 0$ (see the inset of Fig. 5). Fits to Eq. (8) yield $\sigma_* = 3.03(3)$ and $\theta = 0.64(4)$. The scaling form (8) implies that, in the limit $h \rightarrow 0$ and for fixed σ , $M_\infty(t)$ is discontinuous at σ_* . More precisely, as $h \rightarrow 0$, one finds $M_\infty(t) \rightarrow -M_0$ for $\sigma < \sigma_*$, and $M_\infty(t) \rightarrow +M_0$ for $\sigma > \sigma_*$, where M_0 denotes the spontaneous magnetization [47]. The approach to these limiting values is governed by corrections decreasing as h^θ .

We now show that the time $t_*(h) = \exp \sqrt{\sigma_*/h}$, corresponding to the crossing value σ_* , can be related to the critical time $t_c(h)$. In Table I we report $\sigma_c = h(\ln t_c)^2$ and $\hat{\sigma}_c = (\sigma_c - \sigma_*)h^{-\theta}$, which is approximately constant within errors. This implies that $t_*(h) = t_c(h)(1 - bh^\theta)$ with $b = \hat{\sigma}_c/(2\sigma_*) = 0.45(2)$. Therefore, for $h \rightarrow 0$ also t_c diverges as

$$t_c(h) = t_*(h) = \exp \sqrt{\sigma_*/h}. \quad (9)$$

The exponent θ controls the approach to $h = 0$. It is thus natural to conjecture that also the h -dependence of w is controlled by θ , thus $w \propto h^\theta$. Data are consistent: Fits of $w(h)$ to ah^α give $\alpha = 0.60(2)$ (including all values of h) and $\alpha = 0.72(8)$ (discarding the result for $h = 0.07$).

In conclusion, we report a study of the out-of-equilibrium relaxational dynamics arising from quenches of the magnetic field across the low-temperature first-order transition line of the 2D Ising model, at fixed $\beta > \beta_c$ and for several values of the post-quench field $h > 0$. Our results reveal the emergence of a dynamic percolation transition at a finite post-quench critical time t_c , which is marked by the simultaneous percolation of the largest positive cluster and inverse percolation of the largest negative one. For times t close to t_c , the largest-cluster sizes show the expected FSS behavior [see Eq. (5)], in terms of the fractal dimensions d_\pm

and of a critical exponent w controlling the approach to criticality. We find that the fractal dimensions d_\pm are equal, apparently independent of h , and consistent with the RP value $d_{\text{RP}} = 91/48$. On the other hand, the exponent w , controlling the approach to criticality, retains a nontrivial dependence on the post-quench h , and differs from the RP value $w_{\text{RP}} = 3/4$. We find $w < w_{\text{RP}}$ for all considered values of h , with w decreasing as h is reduced, apparently vanishing as $w \sim h^\theta$. From a renormalization-group point of view, this behavior may be interpreted as a line of h -dependent fixed points sharing the same metric (magnetic, in the equivalent spin representation) critical exponents, but differing in the scaling behavior governing the dynamical approach to criticality.

The critical percolation time t_c is related to the typical time t_* at which the system switches from the metastable negatively magnetized phase to the positively magnetized one, and therefore to the spinodal-like behavior of the magnetization in the small- h limit. This implies that the percolation time t_c exhibits a spinodal-like exponential dependence on h , cf. Eq. (9), somehow mimicking the decay of a false vacuum. Our results suggest that the mechanism driving the transition from the metastable to the stable phase is not the independent growth of isolated droplets, but rather their collective aggregation dynamics, whereby droplets predominantly grow through merging processes (see App. A 3).

The percolative behavior outlined in this work is most likely generic. Indeed, percolation transitions are also expected under alternative quenching protocols—such as slowly varying h across the transition point $h = 0$ (see, e.g., Refs. [40, 44–46])—and in higher dimensions. However, in three-dimensional Ising systems the pattern turns out to be quite different [49]: positive and negative clusters undergo separate percolation transitions, with an intermediate dynamical phase in which percolating clusters of both signs coexist. More generally, percolation transitions are expected in systems with discrete symmetries (systems with continuous symmetries may behave differently, due to the presence of long-distance Goldstone-like modes [50]), with features that may depend on the dimensionality and the number of low-temperature phases. Percolation may also be relevant at thermal first-order transitions, such as those occurring in q -state Potts models for large q (some indications in this direction can already be found in the results reported in Ref. [40]). These issues call for further investigation.

We finally remark that the out-of-equilibrium percolation transitions across magnetic first-order transitions represent a new type of non-RP percolative behavior, which naturally emerges in physical systems governed by physically realizable local dynamics. This should be contrasted with other examples of non-RP percolation transitions arising from nonlocal and irreversible *ad hoc* dynamical rules, as in certain network-growth models exhibiting EP transitions [13–35].

Appendix A

Here we report some additional details on the dynamics and quenching protocol, and on the determination of the infinite-volume magnetization $M_\infty(t)$. Moreover, we summarize the arguments leading to the definition of the scaling variable $\sigma = h(\ln t)^2$ [cf. Eq. (7)].

1. Dynamics and quenching protocol

We analyze the out-of-equilibrium evolution arising from a sudden quench of the magnetic field across the low-temperature first-order transition line, at fixed $\beta > \beta_c$. We consider the single-spin heat-bath dynamics, an example of a purely relaxational dynamics [36]: at each site, a new spin is chosen using the conditional probability distribution $P \sim e^{-H(\beta, h)}$ at fixed neighboring spins. Spins are updated using a checkerboard scheme: we first update all spins at even sites, then all spins at odd sites. A time unit corresponds to a complete lattice sweep. The resulting dynamics is not strictly reversible, as the two sublattices are updated sequentially. This also implies that the time t can only take integer values. A reversible dynamics could be obtained by randomly choosing spins at each step. This choice, giving rise to a slightly slower dynamics (the typical time scales differ by a factor of approximately four [51]), would also allow for noninteger values of the time variable. Indeed, if the time unit corresponds to L^2 spin updates, so as to obtain a well-defined infinite-volume limit at fixed t , one might consider time steps of order $1/L^2$. In the $L \rightarrow \infty$ limit, this naturally leads to a continuous-time evolution.

The quenching protocol starts at $t = 0$ from equilibrated negatively magnetized configurations at $\beta > \beta_c$ and $h = 0$. The volume is large enough, so we are effectively considering $h_i = 0^-$ in the thermodynamic limit. Indeed, for $h = 0$, the typical time needed to make a transition from the negative phase to the opposite one scales as $L^2 \exp(2\beta\kappa L)$, where κ is the planar interface tension (see, e.g., Ref. [51]). In particular, for $\beta = 1.2\beta_c$, it scales as $L^2 \exp(0.666L)$, corresponding to 3×10^{68} for $L = 200$. Since we only consider lattices with $L \geq 200$, transitions never occur and therefore the starting configurations have been simply obtained by performing a heat-bath Monte Carlo simulation at $h = 0$, starting from a configuration with $s_{\mathbf{x}} = -1$ for all values of \mathbf{x} . We note that starting from configurations equilibrated at negative values of h would not change the general picture and would only lead to a shift of the critical time t_c .

2. Additional numerical details

In our numerical study we discuss the scaling behavior of the infinite-volume magnetization $M_\infty(t)$ at fixed h . To determine it for a given value of h , we increase L

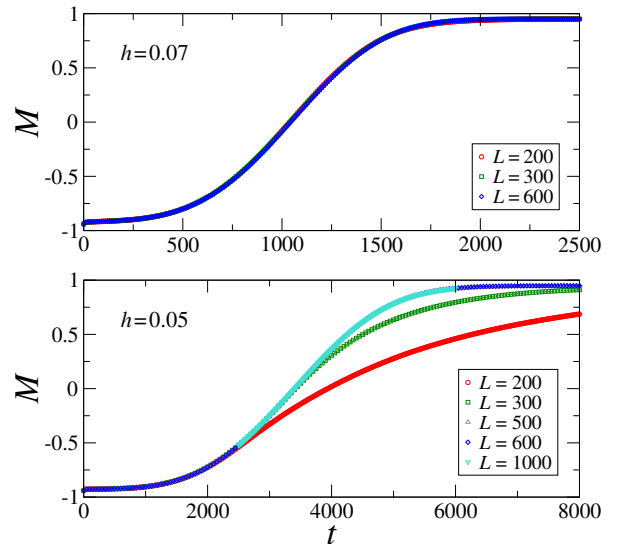


FIG. 6: Time evolution of the magnetization $M(t)$ for $h = 0.07$ (top) and $h = 0.05$ (bottom) and several sizes L . Statistical errors are hardly visible (for $L = 600$, the errors are at most 0.003 and 0.004 for $h = 0.07$ and $h = 0.05$, respectively). Data clearly converge to a limiting curve as L increases, which provides a good approximation of $M_\infty(t)$.

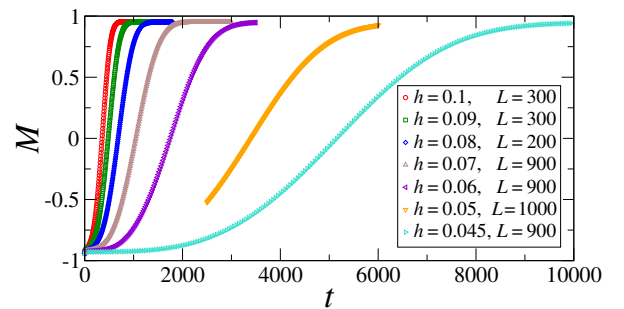


FIG. 7: Time dependence of $M(t)$ for several values of h , and sufficiently large L to provide their infinite-volume limit $M_\infty(t)$ (statistical errors are hardly visible).

until the average magnetization curves become approximately L -independent. The curves corresponding to the largest L then provide the infinite-size $M_\infty(t)$ for the given values of h . As an example, in Fig. 6 we show the magnetization data for two values of h and different lattice sizes. For $h = 0.07$, simulations on lattices of size $L = 200$ already provide the infinite-volume magnetization curves. As h decreases, finite-size effects become larger. For example, for $h = 0.05$ (see Fig. 6), the large- L limit (within errors) is obtained for $L \gtrsim 600$ ($L \gtrsim 900$ for $h = 0.045$). The infinite-volume results for different values of h are reported in Fig. 7 for values of h in the interval $[0.045, 0.10]$. For $h = 0.10$, the transition to the positively magnetized phase occurs rapidly and indeed, for larger values of h , it is difficult to identify an out-of-equilibrium regime. As h decreases, the system persists in the negatively magnetized state for an increasingly

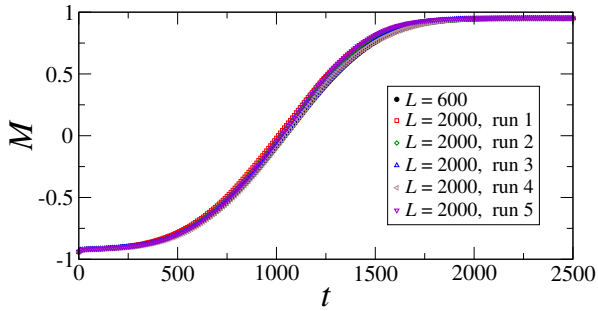


FIG. 8: Comparison of the average magnetization $M(t)$ for $L = 600$ with the instantaneous magnetization for five different runs on a large lattice with $L = 2000$, for $h = 0.07$.

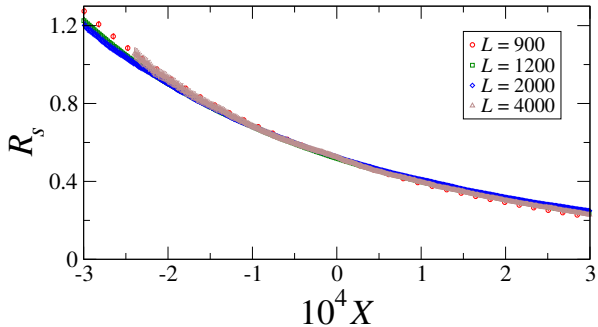


FIG. 9: The ratio R_s vs $X = (t - t_c)L^w$ for $h = 0.045$, with $t_c = 5921$ and $w = 0.52$.

long time interval.

It is important to note that the infinite-volume magnetization curves do not only provide information on the average behavior of the system as a function of t , but represent the evolution of the magnetization of any large system. Indeed, self-averaging holds, so that fluctuations in the evolution vanish for $L \rightarrow \infty$. This is evident from Fig. 8, where we compare the evolution of the instantaneous magnetization on large systems (here $L = 2000$) with the average behavior computed on smaller lattices.

Finally, we report some additional data to support the scaling relation (5). Fig. 9 shows the ratio R_s vs $X = (t - t_c)L^w$ for $h = 0.045$. It is the analogue of Fig. 3, where we report results for $h = 0.07$. Also in this case, data scale quite well.

3. Scaling behavior from droplet nucleation

We outline here the arguments leading to the scaling Ansatz (7) for the magnetization in 2D systems. We assume that, for the infinite-volume dynamics across the

first-order transition line, the relevant scaling variable is the magnetic energy of droplets of positive spins nucleated in the dynamical process, which are eventually responsible for the transition from the metastable negatively magnetized state to the positively magnetized one. Under this hypothesis, the relevant scaling variable is $\sigma \sim hR(t)^d$ (d is the spatial dimension), where $R(t)$ denotes the typical droplet size at time t . Assuming droplets to have smooth boundaries, the time needed to create a droplet of size R should scale as $\exp(cR^{d-1})$ in d dimensions, so $R(t) \sim (\ln t)^{1/(d-1)}$. Therefore we obtain Eq. (7) for $d = 2$.

As discussed in the main text, the scaling of the data in terms of σ implies that for small h the phase change of 2D systems occurs on time scales

$$t_* \sim \exp \sqrt{\sigma_*/h}. \quad (\text{A1})$$

Note that t_* is significantly shorter than the time scale obtained by requiring isolated droplets to be energetically stable. Indeed, the energy of a positive-spin droplet surrounded by negative spins is

$$E = -ahR^d + bR^{d-1}, \quad a, b > 0. \quad (\text{A2})$$

It is immediate to verify that the energy decreases with increasing R , only if R is larger than a threshold R_c that scales as $1/h$. Droplets of size R_c require a time of order $\exp(cR_c) \sim \exp(\bar{c}/h)$ to be generated [39]. For $h \rightarrow 0$, this time scale is significantly larger than the one defined in Eq. (A1), indicating that in two dimensions the transition occurs when typical isolated droplets are too small to be energetically stable. Thus, the main mechanism responsible for the transition in 2D Ising systems is not the independent growth of isolated droplets, but rather their aggregation dynamics: droplets increase their size predominantly by merging, a dynamical process that is always energetically favored. This mechanism allows the system to generate stable positive-spin domains on time scales much shorter than $\exp(\bar{c}/h)$ and is responsible for the percolation transition that marks the passage from one phase to the other.

The relevance of the merging dynamics in the critical region is particularly evident in Fig. 2, where we report the configurations of the system at three different times in the critical region: we consider $t = t_c - 30, t_c, t_c + 30$, with $t_c = 1174$ (results are for $h = 0.07$). In this short time interval, the cluster boundaries barely move and the large increase in the size of the largest positive cluster (Σ_+ approximately takes the values 0.37, 0.50, and 0.64, as time increases) is due to the merging of the largest cluster with smaller positive-spin clusters.

[1] D. Stauffer and A. Aharony, *Introduction to percolation theory* (Taylor and Francis, London, 1994).

[2] M. Sahimi, *Applications of percolation theory* (CRC Press, 1994).

- [3] A. A. Saberi, Recent advances in percolation theory and its applications, *Phys. Rep.* **578**, 1 (2015).
- [4] K. G. Wilson, The renormalization group and critical phenomena, *Rev. Mod. Phys.* **55**, 483 (1983).
- [5] K. G. Wilson and J. B. Kogut, The renormalization group and the epsilon expansion, *Phys. Rep.* **12**, 75 (1974).
- [6] M. E. Fisher, The renormalization group in the theory of critical behavior, *Rev. Mod. Phys.* **46**, 597 (1974); Erratum: *Rev. Mod. Phys.* **47**, 543 (1975).
- [7] F. J. Wegner, The Critical State, General Aspects, C. Domb, C. and M. S. Green editors, *Phase transitions and critical phenomena*, vol. 6, (Acad. Press, London, 1976).
- [8] A. Pelissetto and E. Vicari, Critical phenomena and renormalization group theory, *Phys. Rep.* **368**, 549 (2002).
- [9] H. Kesten, *Percolation Theory for Mathematicians*, (Birkhäuser, 1982).
- [10] S. Smirnov, Critical percolation in the plane: Conformal invariance, Cardy's formula, scaling limits, *C. R. Acad. Sci. (Paris) I* **333**, 239 (2001).
- [11] F. Y. Wu, The Potts model, *Rev. Mod. Phys.* **64**, 235 (1982).
- [12] M. E. J. Newman and R. M. Ziff, Efficient Monte Carlo algorithm and high-precision results for percolation, *Phys. Rev. Lett.* **85**, 4104 (2000); A fast Monte Carlo algorithm for site or bond percolation, *Phys. Rev. E* **64**, 016706 (2001).
- [13] D. Achlioptas, R. M. D'Souza, and J. Spencer, Explosive percolation in random networks, *Science* **323**, 1453 (2009).
- [14] R. M. Ziff, Explosive growth in biased dynamic percolation on two-dimensional regular lattice networks, *Phys. Rev. Lett.* **103**, 045701 (2009).
- [15] Y. S. Cho, J. S. Kim, J. Park, B. Kahng, and D. Kim, Percolation transitions in scale-free networks under the Achlioptas process, *Phys. Rev. Lett.* **103**, 135702 (2009).
- [16] F. Radicchi and A. Fortunato, Explosive percolation in scale-free networks *Phys. Rev. Lett.* **103**, 168701 (2009).
- [17] R. M. Ziff, Scaling behavior of explosive percolation on the square lattice, *Phys. Rev. E* **82**, 051105 (2010).
- [18] R. A. Costa, S. N. Dorogovtsev, A. V. Goltsev, and J. F. F. Mendes, Explosive percolation transition is actually continuous, *Phys. Rev. Lett.* **105**, 255701 (2010).
- [19] R. M. D'Souza and M. Mitzenmacher, Local cluster aggregation models of explosive percolation, *Phys. Rev. Lett.* **104**, 195702 (2010).
- [20] F. Radicchi and S. Fortunato, Explosive percolation: A numerical analysis, *Phys. Rev. E* **81**, 036110 (2010).
- [21] W. Chen and R. M. D'Souza, Explosive percolation with multiple giant components, *Phys. Rev. Lett.* **106**, 115701 (2011).
- [22] J. Nagler, A. Levina, and M. Timme, Impact of single links in competitive percolation, *Nat. Phys.* **7**, 265 (2011)
- [23] P. Grassberger, C. Christensen, G. Bizhani, S.-W. Son, and M. Paczuski, Explosive percolation is continuous, but with unusual finite size behavior, *Phys. Rev. Lett.* **106**, 225701 (2011).
- [24] Y. S. Cho and B. Kahng, Suppression effect on explosive percolation, *Phys. Rev. Lett.* **107**, 275703 (2011).
- [25] H. K. Lee, B. J. Kim, and H. Park, Continuity of the explosive percolation transition, *Phys. Rev. E* **84**, 020101(R) (2011).
- [26] O. Riordan and L. Warnke, Explosive percolation is continuous, *Science* **333**, 322 (2011).
- [27] O. Riordan and L. Warnke, Achlioptas processes are not always self-averaging, *Phys. Rev. E* **86**, 011129 (2012).
- [28] J. Nagler, T. Tiessen, and H. W. Gutch, Continuous percolation with discontinuities, *Phys. Rev. X* **2**, 031009 (2012).
- [29] R. A. da Costa, S. N. Dorogovtsev, A. V. Goltsev, and J. F. F. Mendes, Critical exponents of the explosive percolation transition, *Phys. Rev. E* **89**, 042148 (2014).
- [30] N. Bastas, P. Giazitzidis, M. Maragakis, and K. Kosmidis, Explosive percolation: Unusual transitions of a simple model, *Physica A* **407**, 54 (2014).
- [31] R. M. D'Souza and J. Nagler, Explosive percolation: Novel critical and supercritical phenomena, *Nat. Phys.* **11**, 531 (2015).
- [32] S. Boccaletti, J. A. Almendral, S. Guan, I. Leyva, Z. Liu, I. Sendiña-Nadal, Z. Wang, and Y. Zou, Explosive transitions in complex networks structure and dynamics: Percolation and synchronization, *Phys. Rep.* **660**, 1 (2016).
- [33] M. K. Hassan and M. M. H. Sabbir, Product-sum universality and Rushbrooke inequality in explosive percolation, *Phys. Rev. E* **97**, 050102 (2018).
- [34] M. Li, J. Wang, and Y. Deng, Explosive percolation obeys standard finite-size scaling in an event-based ensemble, *Phys. Rev. Lett.* **130** 147101 (2023).
- [35] L. Yang and M. Li, Emergence of biconnected clusters in explosive percolation, *Phys. Rev. E* **110**, 014122 (2024).
- [36] K. Binder, Monte Carlo investigations of phase transitions and critical phenomena. *Phase Transitions and Critical Phenomena*, Domb, C. & Green, M. S. (eds.) vol. 5b, 1 (Academic Press, London, 1976).
- [37] K. Binder, Theory of first-order phase transitions, *Rep. Prog. Phys.* **50**, 783 (1987).
- [38] A. J. Bray, Theory of phase-ordering kinetics, *Adv. Phys.* **43**, 357 (1994).
- [39] P. A. Rikvold, H. Tomita, S. Miyashita, and S. W. Sides, Metastable lifetimes in a kinetic Ising model: Dependence on field and system size, *Phys. Rev. E* **49**, 5080 (1994).
- [40] A. Pelissetto and E. Vicari, Dynamic off-equilibrium transition in systems slowly driven across thermal first-order transitions, *Phys. Rev. Lett.* **118**, 030602 (2017).
- [41] H. Panagopoulos, A. Pelissetto, and E. Vicari, Dynamic scaling behavior at thermal first-order transitions in systems with disordered boundary conditions, *Phys. Rev. D* **98**, 074507 (2018).
- [42] P. Fontana, Scaling behavior of Ising systems at first-order transitions, *J. Stat. Mech.* 063206 (2019).
- [43] F. Corberi, L. F. Cugliandolo, M. Esposito, O. Mazzarisi, and M. Picco, How many phases nucleate in the bidimensional Potts model?, *J. Stat. Mech.* 073204 (2022).
- [44] A. Pelissetto and E. Vicari, Scaling behaviors at quantum and classical first-order transitions, in *Fifty Years of the Renormalization Group*, Chap. 27, dedicated to the memory of Michael E. Fisher, edited by A. Aharony, O. Entin-Wohlman, D. Huse, and L. Radzihovsky, World Scientific (2024) [arXiv:2302.08238]
- [45] A. Pelissetto and E. Vicari, Out-of-equilibrium spinodal-like scaling behaviors across the magnetic first-order transitions of two-dimensional and three-dimensional Ising systems, *Phys. Rev. E* **113**, 014107 (2026).
- [46] A. Pelissetto, D. Rossini, and E. Vicari, Out-of-equilibrium spinodal-like scaling behaviors at the thermal

- first-order transitions of three-dimensional q -state Potts models, Phys. Rev. E **113**, 024137 (2026).
- [47] C. Itzykson and J.-M. Drouffe, Statistical Field Theory: Volume 1. From Brownian Motion to Renormalization and Lattice Gauge Theory (Cambridge University Press, Cambridge, UK, 1989).
- [48] J. Hoshen and R. Kopelman, Percolation and cluster distribution. I. Cluster multiple labeling technique and critical concentration algorithm, Phys. Rev. B **14**, 3438 (1976).
- [49] A. Pelissetto, D. Rossini, and E. Vicari, in preparation.
- [50] A. Pelissetto and E. Vicari, Off-equilibrium scaling behaviors driven by time-dependent external fields in three-dimensional $O(N)$ vector models, Phys. Rev. E **93**, 032141 (2016).
- [51] A. Pelissetto and E. Vicari, Dynamic finite-size scaling at first-order transitions, Phys. Rev. E **96**, 012125 (2017).